IOP Conference Series: Earth and Environmental Science

PAPER • OPEN ACCESS

Numerical Study on the Propagation Law of Shock Wave in Turning Tunnel

To cite this article: Beilei Zhao *et al* 2019 *IOP Conf. Ser.: Earth Environ. Sci.* **237** 032055

IOP Conf. Series: Earth and Environmental Science **237** (2019) 032055 doi:10.1088/1755-1315/237/3/032055

Numerical Study on the Propagation Law of Shock Wave in Turning Tunnel

Zhao Beilei[1], Zhao Jiguang [2], Cui Cunyan[1*] and Wang Yan[1]

[1]Department of Aerospace Science and Technology, Space Engineering University, Beijing 101416, China

[2] Department of Electronic and Optical Engineering, Space Engineering University, Beijing 101416, China

[*]Corresponding author's e-mail: 13661315668@126.com

Abstract. To study the propagation law of the shock wave in turning tunnel, the propagation process of shock wave in underground turning tunnels of 15°, 30°, 45°, 60°, 75° and 90° was simulated based on ANSYS/LS-DYNA. Results show that at the turning corner, the overpressure on the outside wall is 2 times that on the inside wall. According to the overpressure ratio criterion, the length of the turbulent zone is no more than 3.2 times the equivalent diameter of the tunnel. With the increase of the turning angle, the attenuation coefficient of shock wave decreases gradually, which indicates that the overpressure attenuation becomes less obvious. The results can provide an important reference for the protection design of the turning tunnel.

1. Introduction

The turning tunnel is a common underground tunnel. Once an accidental explosion occurs, the shock wave will propagate along the turning tunnel, which poses a great threat to the facilities and personnel in the tunnel. It is of great significance for protection design to study the propagation law of shock wave in turning tunnel.

The prototype experiment of explosion in a tunnel has the defects of high cost, poor repeatability and serious damage. Scholars at home and abroad mainly carry out the model experiment and numerical simulation. The former Soviet scholar Savanko[1] performed experiments through miniature pipes and found that the shock wave pressure decreased slightly after passing the 90°turning pipe. Igra. O et al.[2] carried out experiments in a supersonic 90°turning pipe with the size of 102 mm×178 mm. Results showed that the shock wave attenuation was accelerated by the diffraction at the turning corner and the turbulence after the turning corner. Wang Yunyan et al.[3] carried out numerical simulations to study the propagation characteristics of shock wave passing through 45° turning tunnel by ANSYS/LS-DYNA finite element software. Wang Lai et al.[4] simulated with the method of fluid grid and obtained the flow field before and after a 90° turning corner. However, the above literatures are limited to a specific turning angle and lack an analysis of shock wave propagation in different turning tunnels. Therefore, the applicability of the conclusions is limited.

Numerical simulations were carried out for six typical turning tunnels of 15°, 30°, 45°, 60°, 75° and 90° using ANSYS/LS-DYNA. The propagation characteristics of shock wave at the turning corners were analysed. The length of turbulent zone after turning corner was investigated and the effect of the turning angle on attenuation coefficient was explored.

IOP Conf. Series: Earth and Environmental Science **237** (2019) 032055 doi:10.1088/1755-1315/237/3/032055

2. Establishment and verification of simulation model

2.1 Establishment of simulation model

The length of the underground tunnel is 82 m and the cross section is rectangular with the size of 3.5 m×8.5 m. The thickness of the tunnel wall is 0.75 m. The tunnel begins to turn at a distance of 40 m from the tunnel entrance. The turning angle α refers to the angle between the tunnel and the positive direction of the *z* axis. The simulation model is shown in Figure 1.

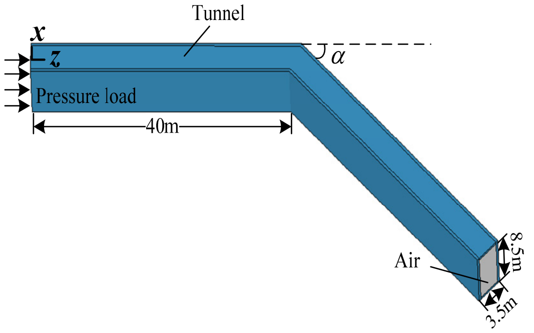

Figure 1. Sinulation model of the turning tunnel.

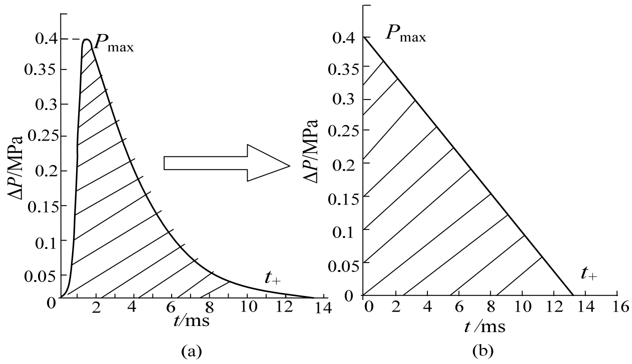

Figure 2. Simplification of the explosive load.

In the actual explosion, the explosive load rises from zero to peak overpressure instantaneously leading to a large error between the calculation steps. The triangular pressure load which descends linearly from the maximum value to zero is usually adopted to decrease this error [4]. The peak overpressure and positive pressure impulse are two important parameters to evaluate the damage effect on the tunnel. According to the principle of “the same peak overpressure and positive pressure impulse”, the exponential explosive load is simplified as a triangular pressure load with the overpressure of 0.4 MPa and positive pressure duration of 13.2 ms, as shown in Figure 2. The pressure load is applied to the normal line of the tunnel entrance.

The model is made up of air and tunnel. The air is modelled using the constitutive equation of MAT_NULL and the state equation of EOS_LINEAR_POLYNOMIAL. The parameters are shown in Table 1[5], in which ρ is density, C_1～C_6 are parameters of the state equation, E_0 is the initial internal energy, V_0 is initial relative volume.

Table 1. Material parameters of the air.

ρ(g/cm^3)	C_1	C_2	C_3	C_4	C_5	C_6	E_0(MPa)	V_0
1.29	0	0	0	0.4	0.4	0	0.25	1.0

The material of the tunnel wall is reinforced concrete, which is described by the material model of MAT_BRITTLE_DAMAGE. The parameters are shown in Table 2[5], in which E is Young’s modulus, v is Poisson ratio, ε_t is tensile limit, ε_s is shear limit, σ_s is compressive yield stress.

Table 2. Material parameters of the tunnel wall.

ρ(g/cm^3)	E(MPa)	v	ε_t (MPa)	ε_s (MPa)	σ_s (MPa)
2.55	2.5×10^4	0.30	3.10	14.48	28.96

The Lagrange grid is built for the tunnel, the Euler grid is built for the air, and the two are coupled through the ALE algorithm. The mesh sizes of the air and tunnel wall are 4 cm and 2 cm respectively. The computing time size is 0.6 μs. The non-reflecting boundary is applied to the air interfaces to prevent the shock wave from re-entering the air field. The explosive energy absorbed by the reinforced concrete wall is ignored and the rigid boundary is set by restraining the normal motion of the particle on the wall. In addition, it is difficult to quantify the roughness of tunnel wall and it is considered as the smooth wall[7].

2.2 Model verification

Oblique reflection occurs when the blast wave hits the tunnel wall at the angle of φ_0. The angle between the reflected shock wave and tunnel wall is φ_2, as shown in Figure 3. The region “I” represents the undisturbed region, the region “II” represents the region where the incident wave has passed but the reflected wave has not, the region “III” represents the region where the reflected wave has passed. D_1 is the velocity of the incident shock wave. u_0, u_1 and u_2 denote the gas velocity in “I”, “II” and “III” areas respectively[8].

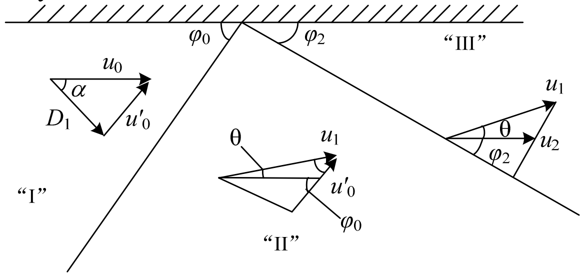

Figure 3. Oblique reflection of shock wave on tunnel wall

When the shock wave passes through the air, the airflow deflects toward the wall, but the velocity component parallel to the shock front remains unchanged.

$$u_0 \cos\varphi_0 = u_1 \cos(\varphi_0 - \theta) \tag{1}$$

For both sides of incident wave, the mass and momentum conservation are obtained:

$$\rho_0 u_0 \sin\varphi_0 = \rho_1 u_1 \sin(\varphi_0 - \theta) \tag{2}$$

$$P_0 + \rho_0 u_0^2 \sin^2\varphi_0 = P_1 + \rho_1 u_1^2 \sin^2(\varphi_0 - \theta) \tag{3}$$

For both sides of the reflected shock wave:

$$u_2 \cos\varphi_2 = u_1 \cos(\varphi_2 + \theta) \tag{4}$$

$$\rho_2 u_2 \sin\varphi_2 = \rho_1 u_1 \sin(\varphi_2 + \theta) \tag{5}$$

$$P_2 + \rho_2 u_2^2 \sin^2\varphi_2 = P_1 + \rho_1 u_1^2 \sin^2(\varphi_2 + \theta) \tag{6}$$

The formula of reflection wave overpressure is obtained by adding the adiabatic equations of incident wave and reflected wave:

$$\Delta P_2 = (1 + \cos\varphi_0)\Delta P_1 + \frac{6\Delta P_1^2 \cos^2\varphi_0}{\Delta P_1 + 7P_0} \tag{7}$$

Where, ΔP_1 is the overpressure of incident wave; ΔP_2 is the overpressure of reflected wave.

Simulation results show that the shock wave overpressure at 40 m form the tunnel entrance is 0.190 MPa, which is regarded as ΔP_1 on the outside wall at the turning corner. The corresponding ΔP_2 is solved by substituting ΔP_1 and the incident angle φ_0 into formula (7). At the same time, according to six groups of simulation results, the overpressure of reflected wave $\Delta P_2'$ on the outside wall at the turning corner is obtained. The theoretical calculation results ΔP_2 are compared with the simulation results $\Delta P_2'$ and the relative errors δ are analyzed, as shown in Table 3. ΔP_2 are larger than $\Delta P_2'$ in six turning tunnels. The influence of the transmitted wave is not considered in the deduction process of theoretical formulas. However, the transmitted wave enters the wall in the simulation process, which leads to the decrease of the wave front energy. The relative errors δ between theoretical and simulation results are less than 10%, which is in an acceptable range. The effectiveness of the simulation model is verified.

Table 3. Comparison of the theoretical and simulation results.

α/°	15°	30°	45°	60°	75°
ΔP_2/MPa	0.318	0.402	0.518	0.634	0.697
$\Delta P_2'$/MPa	0.296	0.380	0.492	0.607	0.664
δ/%	6.918	5.472	5.019	4.259	4.735

3. Simulation results and analysis

3.1 Propagation characteristics of shock waves at turning corner

Figure 4 shows the pressure cloud map of shock wave in 45° turning tunnel at different times. Before the turning tunnel, the propagation of shock wave is consistent with that in the long straight tunnel. The propagation characteristics of shock wave change after the turning corner. The shock wave flows around the protruding corner of the inside wall, the wave front bends and deforms. As a result, the diffraction phenomenon occurs and a clockwise vortex generates. The vortex is composed of a series of expansion waves and the pressure is obviously reduced. At the same time, the shock wave moving along the outside side is blocked by the inclined wall, and the airflow is refracted and reflected. The incident wave and reflected wave superimpose to form a local high pressure region, as shown in Figure 4(a).

When the wave passes through the corner, it propagates in the shape of circular arc and reflects back and forth between the two sides of the wall. The local high pressure region also transmits back and forth. The pressure field is confused and the turbulent region is formed. The tunnel wall is considered as a smooth wall. The location of the reflection point can be determined by the principle of mirror reflection[9], but it still lags behind the superimposed precursor wave. After four oblique reflections, the circular wave front is close to the plane wave front gradually.

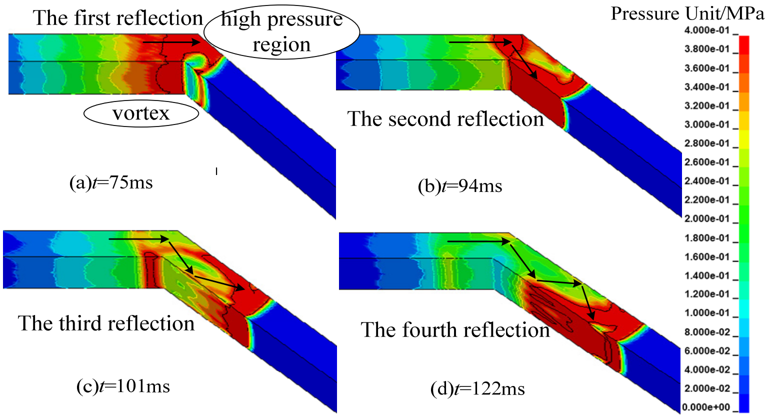

Figure 4. Pressure cloud map in 45° turning tunnel at different times

From the above analysis, it can be seen that under the influence of a series of physical phenomenon, such as flowing around, reflection and superposition, the pressure field at the tunnel corner is disordered and the wave structure is complex. In order to obtain the peak overpressure of shock wave at the corner, A, B and C units were selected on the inside, middle and outside walls respectively. Their position distribution and pressure-time curves are shown in Figure 5. Figure 5 (b) shows that the pressure distribution on the wave front is uneven at the corner, and the pressure increases from the inside wall to the outside wall. The shock wave flows around the inside wall, which produces expansion waves. The interaction between the expansion wave and incident wave reduces the intensity of the wave front. The pressure-time curve of unit A reaches the maximum value of 0.183 MPa and then decays rapidly. The shock wave reflects on the outside wall. The incident wave and reflected wave superimpose, leading to an increase in the intensity of the wave front. The overpressure of unit C reaches 0.492 MPa in a very short time. With the repetition of reflection and superposition, the pressure curve of unit C oscillates several times after a sharp decrease. Unit B is located between the low-pressure and high-pressure regions. Its overpressure is greater than that of unit A and smaller than that of unit C. Its attenuation process is similar to that of unit C. As unit A has no repeated reflection process, its attenuation curve is very smooth.

The overpressures on inside wall, middle wall and outside wall are shown in Figure 6. For different turning angles, the overpressures from the inside to outside wall present a ladder-like change, and the overpressures on the outside wall are about 2～3 times of those on the inside wall. With the increase of turning angle, the shock wave is close to normal reflection on the outside wall, the intensity of the reflected wave enhances continuously and the overpressure on the outside wall increases rapidly. Therefore, the protection of outside wall should be strengthened in the design of turning tunnel, which is consistent with the conclusion in Reference [10].

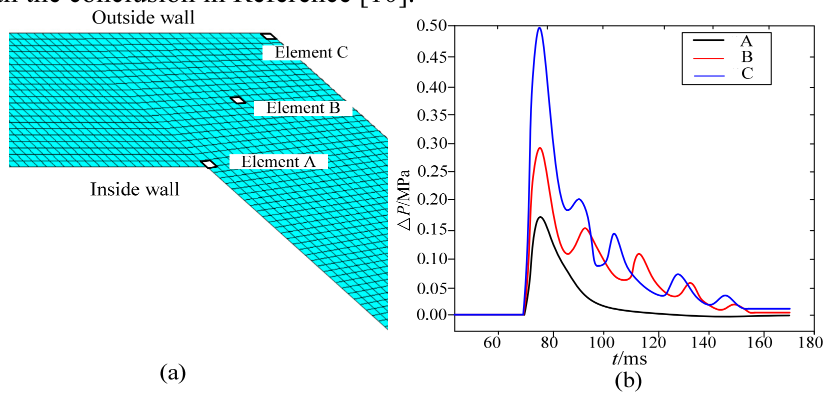

Figure 5. Location distribution and pressure-time curves of three units

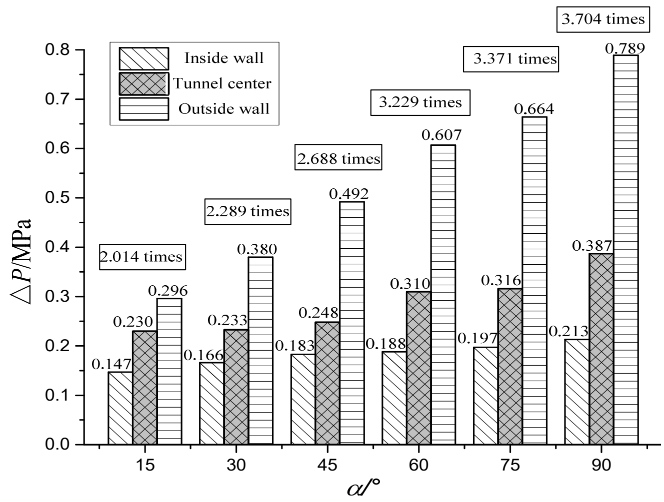

Figure 6. Pressure histogram under different turning angles

3.2 Length of turbulent zone

Shock wave flows around, diffracts and reflects at the tunnel corner leading to a decrease or increase of the local overpressure, the pressure field presents obvious nonlinear characteristics. After the turbulent zone, the shock wave gradually returns to plane wave and its propagation in the tunnel can be approximated to one-dimensional flow. Reference [9] gives a quantitative criteria of $\Delta P_{\max}/\Delta P_{\min} \le 1.5$ for evaluating the plane wave. $\Delta P_{\max}$ and $\Delta P_{\min}$ are the maximum and minimum overpressures of the wave front. When the overpressure ratio satisfies $\Delta P_{\max}/\Delta P_{\min} \le 1.5$, the shock wave can be regarded as a plane wave.

As shown in Figure 7, O_1 is the turning point on the inside wall and the horizontal distance from OO_1 to the tunnel entrance is 40 m. O_1O_2 is the reference plane for measuring the axial distance *s* after the turning corner. A total of 10 parallel planes A_1A_2～J_1J_2 are taken from O_1O_2 at the interval of 4 m. Several measuring points on the plane are selected to get the maximum and minimum overpressure.

The curves of the overpressure ratio $\Delta P_{\max}/\Delta P_{\min}$ versus the axial distance *s* in different turning tunnels are shown in Figure 8. For 15°, 30° and 45° turning tunnels, the shock wave meets the criteria of $\Delta P_{\max}/\Delta P_{\min} \le 1.5$ at D_1D_2 firstly. The shock wave reverts to plane wave at *s*=16 m. For 60°, 75° and 90° turning tunnels, the shock wave meets the criteria of $\Delta P_{\max}/\Delta P_{\min} \le 1.5$ at E_1E_2 firstly. The shock wave reverts to plane wave at s=20 m. Considering that the equivalent diameter of the tunnel is 6.16 m, the maximum length of turbulent zone is 3.2 times the equivalent diameter of the tunnel with the turning angle less than 90°. In the same tunnel, the overpressure ratio of the wave front decays faster in the turbulent zone. The reason is that the flow particles in the turbulent zone mix each other and move disorderly. The shear stress generated in the chaotic flow field accelerates the internal energy dissipation and kinetic energy loss between the fluid layers. When the shock wave restores to a plane wave, the overpressure ratio decays slowly and approaches 1 gradually. The plane wave is still restrained by the wall in the propagation process. It is reflected and superimposed near the wall, resulting in a high intensity around and a low intensity in the middle. Therefore, the overpressure ratio $\Delta P_{max} / \Delta P_{min}$ cannot reach 1 and there is no plane wave with uniform pressure distribution.

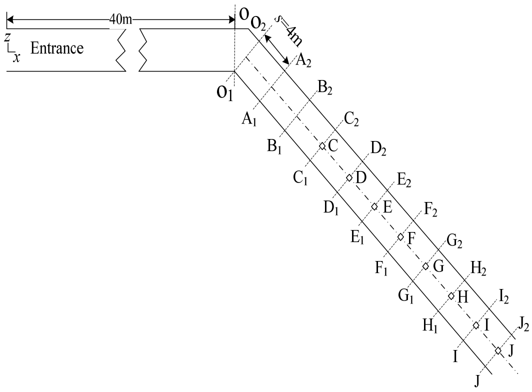

Figure 7. Schematic diagram of plane distribution after the turning corner

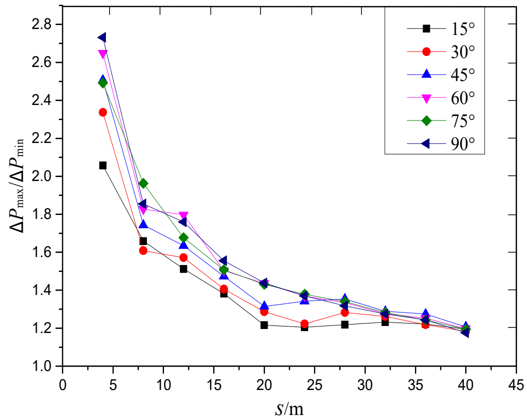

Figure 8. Variation curve of overpressure ratio with axial distance

3.3 Influence of the turning angle on attenuation coefficient

The attenuation coefficient θ_i of shock wave in the turning tunnel is defined as:

$$\theta_i = \frac{\Delta P_0}{\Delta P_{15i}} (i = 1,2,3,4,5,6) \tag{8}$$

Where, ΔP_0 denotes the overpressure of shock wave at a certain position in the long straight tunnel; ΔP_{15i} (i=1,2,3,4,5,6) represents the overpressure of shock wave at the same position of 15°, 30°, 45°, 60°, 75° and 90° turning tunnels respectively.

The attenuation coefficient indicates the attenuation degree of the shock wave passing through the turning tunnel. The larger attenuation coefficient, the more obvious the shock wave attenuation is. In Figure 7, eight measuring points C～J are chosen on the central axis to obtain their overpressures and calculate the attenuation coefficients. The attenuation coefficient θ_i varying with the turning angle α and the axial distance s is shown in Figure 9.It can be seen from Figure 9 that θ_i fluctuates up and down to a certain extent under the influence of reflection and superposition of shock wave in the same turning tunnel, but it shows a downward trend on the whole. The overpressure decreases gradually with the increase of axial distance. This is because the positive pressure zone is widened and more air is compressed. Part of kinetic energy is converted into the internal energy of air. Meanwhile, irreversible energy losses such as thermal radiation and heat conduction exist.

The θ_i in different turning tunnels are all greater than 1, indicating that the attenuation of shock wave is more obvious than that in the long straight tunnel. The energy of the wave front is consumed by the physical phenomenon such as flowing around, diffraction, expansion and the chaotic motion of the particles in the turbulent zone. Although the intensity of wave front is enhanced and the energy is supplemented to a certain extent by the reflection and superposition on the wall, the energy dissipation is larger than complement on the whole. The turning angle increases from 15° to 90°, the attenuation coefficient decreases from 1.26~1.13 to 1.12~1.04. The closer the turning angle is to 90°, the stronger the reflection of shock wave on the wall is, the more energy the wave front receives, and the less obvious the overpressure attenuation is.

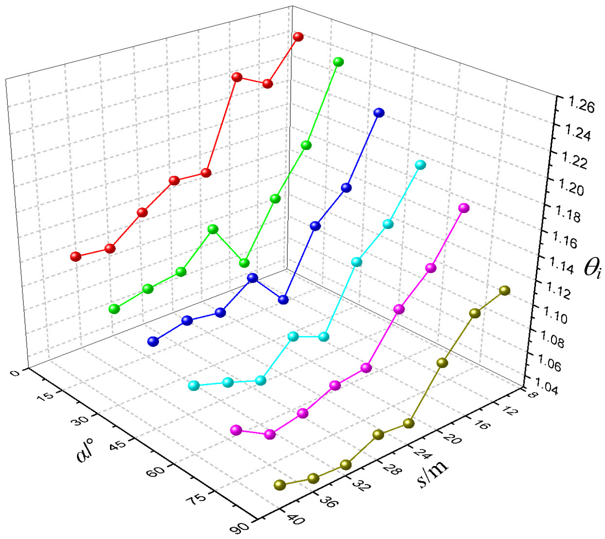

Figure 9. Three dimensional curve of θ_i changing with α and s

4. Conclusions

The propagation processes of shock wave in 15°, 30°, 45°, 60°, 75° and 90° turning tunnels were simulated. The propagation characteristics at the turning corner were analyzed. The influence of turning angle on the length of turbulent zone and attenuation coefficient was studied.

(1) At the turning corner, the overpressure on the inside wall is the minimum and the pressure on the outside wall is the maximum. the overpressures on the outside wall are about 2～3 times of those on the inside wall when α is 15°, 30°, 45°, 60°, 75°, 90°.

(2) After the shock wave passing the turning corner, a turbulent zone is formed, and it returns to the plane wave gradually. The length of the turbulent zone does not exceed 3.2 times the equivalent diameter of the tunnel.

(3) When the turning angle increases from 15° to 90°, the attenuation coefficient decreases from 1.26~1.13 to 1.12~1.04, the attenuation of shock wave overpressure becomes less obvious.

References

[1] Savanko, C.K., Long W.Q.(1979) Shock Wave in the Pit. Metallurgical Industry Press, Beijing.
[2] Igra, O., Falcovitz, J., Houas, L. (2013) Review of methods to attenuate shock waves. Progress in Aerospace Sciences, 58:1-35.
[3] Wang, Y.Y., Qin, B., Zhang, Q. (2007) Characteristic propagation features of the explosion air shock wave at the corner of tunnel. Journal of safety and environment, 7(3):105-107.
[4] Li, Z.X., Shi, Y.C. (2015) Blast Analysis of Building Structures. Science Press, Beijing.
[5] Livemore Software Technology Corporation. (2003) LS-DYNA Keyword Use's Manual. Livemore software Technology Corporation, California.
[6] Liu, J.B., Yan, Q.S., Wu, J. (2009) Analysis of blast wave propagation inside tunnels. Journal of Vibration and Shock, 28(6):8-11.
[7] Li, X.C., Nie, B.S., Yang, C.L., et al. (2017) Effect of gas concentration on kinetic characteristics of gas explosion in confined space. Chinese Journal of High Pressure Physics, 31(2): 135-144.
[8] Luo, T.Q. (2007) Fluid Mechanics. Machinery Industry Press, Beijing.
[9] Qin, B., Zhang, Q., Xiang, C., et al. (2008) Research on the shockwave turbulence area inside the turning tunnel by numerical simulation. Metal Mine, 10: 16-20.

[10] Qu, K.K., Yan, Y.J., Liu, Y., et al. (2011) Comparative study on propagation rules of explosive shock-wave in long straight and complex tunnel. Chinese Journal of Applied Mechanics, 28(4): 434-438.